Received: 14 April 2023 | Accepted: 29 September 2023

DOI: 10.1111/fcp.12960

ORIGINAL ARTICLE

Fundamental & Clinical Pharmacology | WILEY

Synthesis, molecular docking, ADMET, and evaluation of the anxiolytic effect in adult zebrafish of synthetic chalcone (*E*)-3-(4-(dimethylamino)phenyl)-1-(2-hydroxyphenyl)prop-2-en-1-one: An in vivo and in silico approach

Larissa Santos Oliveira[1] | **Maria Kueirislene Amâncio Ferreira**[1] | **Francisco Wagner de Queiroz Almeida-Neto**[1] | **Antonio Wlisses da Silva**[2] | **José Ivo Lima Pinto Filho**[3] | **Matheus Nunes da Rocha**[1] | **Emanuelle Machado Marinho**[4] | **Walber Henrique Ferreira Ribeiro**[3] | **Márcia Machado Marinho**[3] | **Emmanuel Silva Marinho**[1] | **Jane Eire Silva Alencar de Menezes**[1] | **Hélcio Silva dos Santos**[1,2,3]

[1]Science and Technology, Graduate Program in Natural Sciences, State University of Ceará, Fortaleza, Ceará, Brazil

[2]Northeast Biotechnology Network, Graduate Program of Biotechnology, State University of Ceará, Fortaleza, Ceará, Brazil

[3]Chemistry Course, State University of Vale do Acaraú, Sobral, Ceará, Brazil

[4]Department of Organic and Inorganic Chemistry, Federal University of Ceará, Fortaleza, Ceará, Brazil

Correspondence
Hélcio Silva dos Santos, Chemistry Course, State University of Vale do Acaraú, Sobral, CE, Brazil.
Email: helciodossantos@gmail.com; helcio.silva@uece.br

Funding information
Conselho Nacional de Desenvolvimento Científico e Tecnológico, Grant/Award Number: 306008/2022-0; Coordenação de Aperfeiçoamento de Pessoal de Nível Superior, Grant/Award Number: 88881.692120/2022-01; Fundação Cearense de Apoio ao Desenvolvimento Científico e Tecnológico, Grant/Award Number: DCT-0182-00048.02.00/21 e 04879791/2022

Abstract

Background: Anxiety disorders represent the complex interaction between biological, psychological, temperamental, and environmental factors; drugs available to treat anxiety such as benzodiazepines (BZDs) are associated with several unwanted side effects. Although there are useful treatments, there is still a need for more effective anxiolytics with better safety profiles than BZDs. Chalcones or 1,3-diphenyl-2-proper-1-ones can be an alternative since this class of compounds has shown therapeutic potential mainly due to interactions with $GABA_A$ receptors and serotonergic system.

Objectives: This study evaluated the anxiolytic potential of chalcone (*E*)-3-(4-(dimethylamino)phenyl)-1-(2-hydroxyphenyl)prop-2-en-1-one (C2OHPDA) in adult zebrafish (*Danio rerio*) (ZFa).

Methods: Each animal ($n = 6$/group) was treated intraperitoneally (i.p.; 20 μL) with the chalcone (4, 20, and 40 mg/kg) and with the vehicle (DMSO 3%; 20 μL), being submitted to the tests of locomotor activity and 96-h acute toxicity. The light/dark test was also performed, and the serotonergic mechanism (5-HT) was evaluated through the antagonists of the 5-HTR_1, 5-$HTR_{2A/2C}$, and 5-$HTR_{3A/3B}$ receptors. It was investigated the prediction of the chalcone's position and preferential orientation concerning its receptor, as well as the pharmacokinetic parameters (ADMET) involved in the process after administration.

Abbreviations: ^{1}H and ^{13}C NMR, hydrogen and carbon-13 nuclear magnetic resonance; 5-HT, 5-hidroxitriptamina; 5-HT1 and 5-HT2A/2C, 5-hydroxytryptamine receptor 1 and receptor 2A/2C; 5-HT2A, 5-hydroxytryptamine receptor 2A; ADMET, absorption, distribution, metabolism and excretion; ANOVA, variance analysis; BBB, blood–brain barrier; C2OHPDA, chalcone (*E*)-3-(4-[dimethylamino]phenyl)-1-(2-hydroxyphenyl)prop-2-en-1-one; $CDCl_3$, CNS MPO, central nervous system multiparameter optimization; CEUA-UECE, Ethics Committee for the Use of Animals of the State University of Ceara; CNS, central nervous system; CWB, co-crystallized inhibitor granisetron; deuterated chloroform; CYP450, cytochrome P450; Cypro, cyproheptadina; DMSO, dimethyl sulfoxide; DZP, diazepam; Flx, fluoxetine; GSK, Veber's rule; GSTN, granisetron hydrochloride; HIA, human intestinal absorption; IAH, intestinal ephitelial cells; LD_{50}, lethal dose capable of killing 50% of the animals; LGA, Lamarckian genetic algorithm; MDCK, Madin–Darby canine kidney cell line; PDB, protein data bank; Pgp, P-glycoprotein substrate; PIZ, pizotifen maleate; RMSD, root mean square deviation; SOMP, site of metabolism prediction; TLC, thin layer chromatography; TPSA, calculated polar surface area; VD, volume of distribution; ZFa, zebrafish.

Results: As a result, C2OHPDA was not toxic and reduced the locomotor activity of ZFa. Furthermore, chalcone demonstrated an anxiolytic effect on the central nervous system (CNS), mediated by the serotonergic system, with action on 5-HT_{2A} and 5-$HTR_{3A/3B}$ receptors. The interaction of C2OHPDA with 5-HT_{2A}R and 5-HT_{3A} receptors was confirmed by molecular docking study, the affinity energy observed was −8.7 and −9.1 kcal/mol, respectively.
Conclusion: Thus, this study adds new evidence and highlights that chalcone can potentially be used to develop compounds with anxiolytic properties.

KEYWORDS
anxiety, chalcone, zebrafish

1 | INTRODUCTION

Chalcones constitute the class of flavonoids. In their chemical structure, they have two aromatic rings linked through a carbonyl group and a conjugated olefin, being an α,β-unsaturated carbonyl system with a basic structure of 1,3-diphenyl-2-propen-1-one. They occur naturally in vegetables, flowers, roots, and fruits [1, 2].

Chemically, chalcones and their derivatives can undergo substitutions in their aromatic rings, being responsible for different spectra of activity. Thus, they have drawn attention for their simple structure associated with several pharmacological activities, such as anticancer [3], anti-inflammatory [4], antibacterial [5], antioxidant [6], antinociceptives [7], analgésicos [8], analgesics [9], antichagasic [10], and anxiolytics [11].

Anxiety is considered a psychic disorder that affects thousands of people around the world. It is an emotion innate to the human being, but when in excess, it becomes a disease. It occurs through a high process of excitation of the central nervous system (CNS), generating unpleasant sensations of tension, fear and restlessness, which are associated with the anticipation of something that may or may not happen [12]. It is estimated that in Brazil, in a survey carried out in 2017, at least 9.3% of the population had anxiety [13], with this number increasing even more during the SARS-CoV-2 pandemic (COVID-19), about 44% of the Brazilian population felt more anxious about the whole situation the world was going through [14]. The best-known anxiolytics are benzodiazepines and barbiturates. However, they have many associated toxic effects, such as sedation, drowsiness, dizziness, vertigo, mood swings, paranoia, irritability, and neurotoxicity [15].

To search for new drugs with anxiolytic effects, several experimental animal models are available for the initial preclinical phase in vivo. Each has its particularities, advantages, and disadvantages. For example, zebrafish (*Danio rerio*) has been widely used recently, as it has a high reproduction rate, ease of handling, small size, transparency, external fertilization, and low cost [16, 17]. Furthermore, its genetic homology with that of humans is 76%, with 82% for disease-related genes. Compared to other animal models, such as mice, which are widely used, their genetic homology is 84% about living beings, a value very close to that of zebrafish [18].

The pharmaceutical industry faces several challenges in drug research and development (R&D), and the high investments that are constantly required are considered high risk [19]. Thus, the molecular docking technique has been gaining prominence in the design of new drugs. Through this technology, it is possible to predict the drug's site of action, in addition to the mechanism involved, reducing costs and making the process more efficient [20]. Recently, it has been used to predict unwanted effects in polypharmacology and drug reuse [21]. The in vitro evaluation of ADMET parameters (absorption, distribution, metabolism, and excretion) is also used as an initial analysis and seeks to investigate whether the drug under study has desirable metabolism and pharmacokinetics, being an essential tool during the screening process [22]. While the in vivo process involves a greater complexity of factors and mechanisms, prediction via ADME is simplified into the most critical components or divided into several unique processes [3].

This study seeks to analyze the anxiolytic pharmacological activity of the chalcone C2OHPDA, duly synthesized and characterized, through in silico tests, such as molecular docking and ADME, and in vivo tests in the zebrafish model, aiming at the high demand for depressant drugs of the CNS, with more specific and less harmful action to the organism.

2 | MATERIALS AND METHODS

2.1 | Synthesis and chemical characterization of chalcone C2OHPDA

The 2-hydroxyacetophenone (2 mmol) and 4-(dimethylamino)benzaldehyde (2 mmol) were placed

in a volumetric flask (25 mL). Then 5 mL of ethanolic NaOH (50%) solution was added and mixed with stirring for 48 h at room temperature. The progress of the reaction was checked by TLC (n-hexane: ethylacetate, 2:1). After 48 h, the reaction mixture was neutralized with dilute HCl (10%) and ice water added. The product was obtained as a yellow solid filtered under reduced pressure, washed with cold water, and recrystallized from ethanol (Scheme 1). ^{1}H and ^{13}C NMR spectra were obtained using a Bruker Spectrometer, model Avance DPX-300, operating at a frequency of 300 MHz for hydrogen and 125 MHz for carbon, respectively. The spectra were measured in $CDCl_3$, and chemical shifts are reported as δ values in parts per million (ppm) relative to $CDCl_3$.

2.2 | Drugs and reagents

The following reagents and drugs were used: diazepam (Teuto), flumazenil (Sandoz), pizotifen maleate (Sandomigran®), granisetron hydrochloride (Kytril), fluoxetine (Teuto), cyproheptadina (Cobavital®), and dimethyl sulfoxide (Dynamic®).

2.3 | General protocol zebrafish

The animals used in the experiments were wild zebrafish (ZFa) (short-finned phenotype), adults, aged 90 to 120 days, sizes 3.5 ± 0.5 cm, and weight 0.4 ± 0.1 g. They were obtained from Agroquímica: Comércio de Produtos Veterinários LTDA, a supplier in Fortaleza (Ceará, Brazil). The ZFa were acclimatized for 24 h in glass aquariums (30 × 15 × 20 cm), containing dechlorinated water (ProtecPlus® antichlorine), air pumps with submerged filters, at 25°C and pH 7.0 and fed with commercial feed (ad libitum) 24 h before the experiments. In the experiments, ZFa of both sexes were chosen at random, transferred to a damp sponge and treated with the test or control sample. The animals ($n = 6$/group) were treated intraperitoneally (i.p.) with C2OHPDA (4, 20 and 40 mg/kg; 20 μL) or vehicle (control; 3% DMSO; 20 μL; i.p.) or diazepam (DZP 4 mg/kg). For intraperitoneal application, an insulin syringe (0.5 mL; UltraFine® BD) with a 30G needle was used [23, 24]. After the experiments, the animals were euthanized by immersion in cold water (2–4°C) until the loss of opercular movements. All experimental procedures were approved by the Ethics Committee for the Use of Animals of the State University of Ceará (CEUA-UECE), under protocol n° 04983945/2021.

2.4 | Acute toxicity to adult zebrafish

To assess the acute toxic effect of chalcone, the fish were treated intraperitoneally with C2OHPDA or vehicle, after the treatments, the animals were acclimatized and kept under observation for analysis of the mortality rate for a period of 96 h, and every After 24 h, the number of dead fish in each group was recorded. The lethal dose capable of killing 50% of the animals (LD_{50}) was determined by the mathematical method Trimmed Spearman-Karber with a confidence interval of 95% [25, 26].

2.5 | Open-field test

To assess whether there was locomotor alteration in the animals caused by chalcone, either by sedation, muscle relaxation, or any effect on the CNS, an open-field test was performed. ZFa were treated intraperitoneally with C2OHPDA or vehicle or diazepam. After 30 min of treatments, the animals were placed in Petri dishes containing the same aquarium water, the petri dishes were marked with two lines drawn from the center to the edges, leaving a cross shape, connecting four quadrants at the end of the markings. Locomotor activity was analyzed by counting the number of line crossings performed by the fish during 5 min of analysis [23].

2.6 | Test light and dark

The investigation of the anxiolytic-like effect of chalcone was carried out through the light and dark test. ZFa were treated intraperitoneally with C2OHPDA or vehicle or diazepam. A Naive group has been included. After 30 min of the treatments, the animals were added to the light zone of the glass aquarium (divided in half into two light and dark zones soured with white and black paper), with drug-free water. The anxiolytic-type effect was identified by blind evaluators by counting the

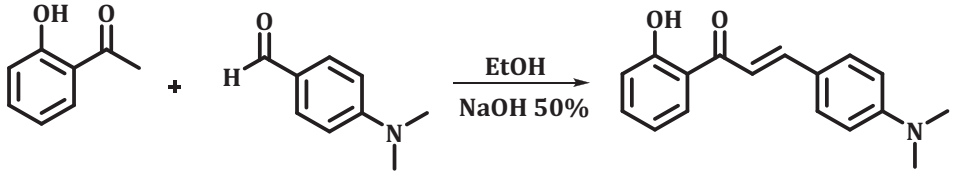

SCHEME 1 Synthesis of chalcone (*E*)-3-(4-(dimethylamino) phenyl)-1-(2-hydroxyphenyl)prop-2-en-1-one.

time the animals spent in the light zone, during 5 min of analysis [27].

2.7 | Involvement of the serotonergic system (5-HT)

To evaluate the mechanism of action of the anxiolytic effect of chalcone (see results), groups of animals ($n = 6$/group) were pretreated with cyproheptadine (5-HT2A antagonist; 32 mg/kg; orally) or pizotifen (5-HT_1 and 5-$HT_{2A/2C}$ antagonist; 32 mg/kg; orally) or granisetron (5-$HT_{3A/3B}$ antagonist, 20 mg/kg; orally), and after 30 min, they received the lowest anxiolytic dose intraperitoneally of C2OHPDA (4 mg/kg) or fluoxetine (Flx; 0.05 mg/kg, i.p.) as a positive control [28]. Subsequently, the animals were taken to the light and dark test as described above.

2.8 | Statistical analysis

After homogeneity and confirmation of normal data distribution, differences between groups were submitted to analysis of variance (ANOVA), followed by Tukey test. Mechanism of action groups were subjected to two-way ANOVA analysis of variance. All results were expressed as mean values ± standard error of mean for each group of six animals. All analyzes were performed with GraphPad Prism v. software. 6.01. The adopted statistical significance level was 5% ($P < 0.05$).

2.9 | Computational details

To carry out the computational simulations, the codes used were Autodocktools ™ [29], AutoDockVina ™ [30], Discovery studio visualizer ™ viewer [31], Gabedit 2.5.0 software [32], Gaussian 09 software [33], MarvinSketch™ (http://www.chemaxon.com) [34], Pymol [35], and UCSF Chimera ™ [36].

2.10 | Ligand design and optimization

The chemical structure of the C2OHPDA was designed using the MarvinSketch code [34], saved at physiological pH (Figure 2). The molecular structure of the C2OHPDA was geometrically optimized by applying the density functional theory method using the Gaussian 09 software [33] at B3LYP/6-311++G(d,p) computational level [37] in the gas phase. From the optimized geometry, the Molecular Electrostatic Potential was computed at the same level of theory, and its isosurface was rendered using the Gabedit 2.5.0 software [32] with an isovalue of 0.01.

2.11 | General docking procedures

To evaluate the mechanism of action of C2OHPDA on 5-HT_{2A}R and 5-HT_{3A} channels, molecular docking simulations were performed, and the structures of the receptors obtained from the Protein Data Bank repository (https://www.rcsb.org/), identified as "Crystal structure of 5-HT_{2A}R in complex with risperidone" (PDB 6A93) [38] and "Cryo-EM structure of 5HT_{3A} receptor in presence of granisetron" (PDB 6NP0) [39]. The preparation of protein structures was performed using the AutoDockTools code [40], where residues were removed and added to Gasteiger charges and polar hydrogen atoms [41].

Fifty independent molecular docking simulations were performed using the AutoDockVina code [30], configured to run the Lamarckian Genetic Algorithm (LGA) and *Exhaustiveness* 64 [42]. The simulation grid was centered on the target to encompass the entire protein structure from the axes: 46155 (x), 1109 (y) and 39 552 (z), with size parameters 118 Å (x), 56 Å (y) and 116 Å (z) with channel 5-HT_{2A}R and axes: 159615 (x), 159 705 (y) and 161 067 (z), size parameters 94 Å (x), 80 Å (y), and 126 Å (z) with channel 5-HT_{3A}, both for the docking simulations of the chalcone C2OHPDA and the redocking simulations of risperidone (8NU) and granisetron (CWB), co-crystallized inhibitors on 5-HT_{2A}R and 5-HT_{3A} targets, respectively. The redocking technique was performed to validate the docking simulations.

Two criteria were used to select the best pose, the first was the statistical parameter root mean square deviation (RMSD), with values up to 2.0 Å considered ideal [43] and the second criterion used was the affinity energy, with values lower than −6.0 kcal/mol being an ideal parameter [44], affinity energy was also used to assess the stability of the receptor-ligand complexes formed. To evaluate the intensity of the hydrogen bonds (H-Bond), the distances between the donor and acceptor atoms were used, where *Strong* bonds present distances between 2.5 and 3.1 Å, *Average* bonds between 3.1 and 3.55 Å, and *Weak* bonds present a greater distance at 3.55 Å [45].

2.12 | Drug-likeness evaluation and ADME properties

With a methodology adapted from Rocha et al. [46], the physicochemical properties of chalcone C2OHPDA were calculated in the academic license software MarvinSketch v21.12, ChemAxon (https://chemaxon.com/products/marvin) to be applied to the criteria drug-likeness of Lipinski's "rule of five" and Veber's rule [47] and optimized by Pfizer's central nervous system multiparameter optimization (CNS MPO) algorithm. The ADMET properties were predicted by the

consensual analysis of the in silico prediction of the SwissADME platform (http://www.swissadme.ch/) and the numerical values of in vitro tests of the ADMETlab v2.0 platform (https://admetmesh.scbdd.com/). Drug-likeness results were plotted on the bioavailability radar, according to the reference [48].

3 | RESULTS AND DISCUSSION

3.1 | Spectroscopic analysis

^{1}H NMR spectrum (Figure 1), the signals at δ_H 7.46 (d, $J = 15.2$ Hz) and 7.92 (d, $J = 15.0$ Hz) are attributed to two doublets referring to the α,β unsaturated hydrogens. The signals at δ_H 7.89–7.94 (m, H6′), 7.0 (d, $J = 8.4$ Hz, H3′) and 7.56–7.59 (m, H4′) and 6.92 (t, $J = 7.2$ Hz, H5′) refer to the aromatic hydrogens of the A ring, and signs at δ_H 7.59 (d, $J = 8.8$ Hz, H3/5) and 7.43–7.48 (d, $J = 8.5$ Hz, H2/6) refer to the aromatic hydrogens of the B ring. In the ^{13}C NMR spectrum (Figure 2), we have the signal referring to the α,β unsaturated carbonyl at δ_C 190.5. The α and β olefinic carbons are seen at δ_C 146.7 and 118.7, respectively. At δ_C 163.6 (C-2′), 135.8 (C-4′), 129.5 (C-6′), 122.2 (C-1′), 118.7 (C-3′), and 118.6 (C-5′), we have the signals referring to the carbons present in ring A, and the signals at δ_C 154.5 (C-4), 132.1 (C-1), 131.0 (C-2/6), and 114.4 (C-3/5) refer to the B ring carbons. The analysis of the spectroscopic data (Table 1) allowed unequivocally to confirm the structure of the compound as being the chalcone (*E*)-3-(4-(dimethylamino)phenyl)-1-(2-hydroxyphenyl)prop-2-en-1-one.

3.2 | Acute toxicity

The chalcone C2OHPDA did not cause any apparent anatomical changes and was not toxic to adult zebrafish up to 96 h of analysis (LD_{50} > 40 mg/kg).

3.3 | Open-field testing

The ANOVA one-way analysis of variance indicated that higher doses of chalcone C2OHPDA (**$P < 0.01$ [20 mg/kg]; ****$P < 0.0001$ [40 mg/kg]) and diazepam [****$P < 0.0001$ (40 mg/kg)] significantly decreased the locomotor activity of the adult zebrafish compared to the control groups (naive and vehicle) (Figure 3).

3.4 | Preliminary anxiety test

The chalcone C2OHPDA increased the time spent in the light region of the aquarium of the animals (****$P < 0.0001$ [4, 20, and 40 mg/kg]), significantly similar to the effect of diazepam (****$P < 0.0001$ [Dzp; 40 mg/kg; i.p.]), which is an anxiolytic behavior in ZFa in the light and dark test (Figure 4).

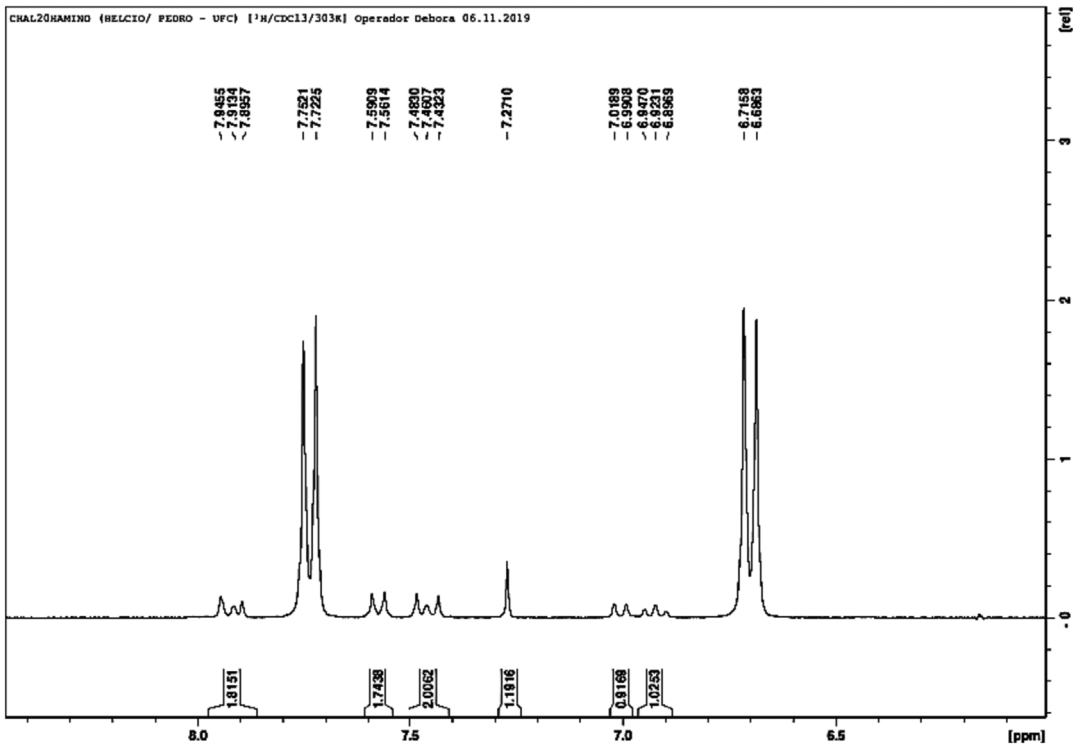

FIGURE 1 ^{1}H NMR spectrum ($CDCl_3$, 300 MHz) of chalcone (*E*)-3-(4-(dimethylamino)phenyl)-1-(2-hydroxyphenyl)prop-2-en-1-one.

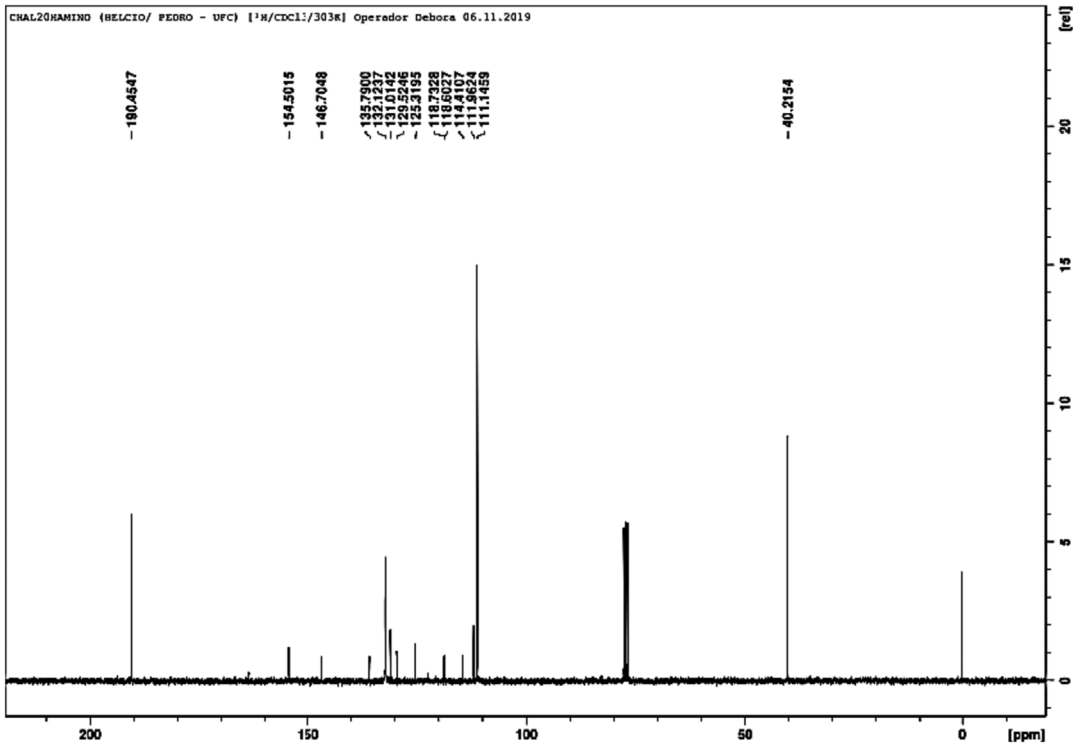

FIGURE 2 ^{13}C NMR spectrum ($CDCl_3$, 125 MHz) of chalcone (*E*)-3-(4-(dimethylamino)phenyl)-1-(2-hydroxyphenyl)prop-2-en-1-one.

TABLE 1 ^{1}H and ^{13}C NMR data of chalcone (*E*)-3-(4-(dimethylamino)phenyl)-1-(2-hydroxyphenyl)prop-2-en-1-one in CDCl3. The chemical shifts in δ_C and δ_H are ppm.

C	δ_C	δ_H
1′	122.4	
2′	163.6	
3′	118.7	7.0 (d, $J = 8.4$ Hz)
4′	135.8	7.56–7.59 (m)
5′	118.6	6.92 (t, $J = 7.2$ Hz)
6′	129.5	7.89–7.94 (m)
C=O	190.5	
1	132.1	
2/6	131.0	7.43–7.48 (d, $J = 8.5$ Hz)
3/5	114.4	7.59 (d, $J = 8.8$ Hz)
4	154.50	
C_α	118.7	7.46 (d, $J = 15.2$ Hz)
C_β	146.7	7.92 (d, $J = 15.0$ Hz)
$2 \times CH_3$	40.2	3.1 (s)

3.5 | Involvement of the serotonergic system (5-HT)

3.5.1 | Involvement of the 5-HT_{2A} system

The two-way ANOVA statistical analysis indicated that pretreatment with cyproheptadine reduced ($^{\#\#}P < 0.01$) the anxiolytic effect of C2OHPDA chalcone (4 mg/kg, i.p.) and also reduced ($^{\#\#\#\#}P < 0.0001$) the anxiolytic effect of fluoxetine (Flx; 0.05 mg/kg; i.p.) (Figure 5a).

3.5.2 | Involvement of 5-$HT_{3A/3B}$ system

Pre-treatment with granisetron reduced ($^{\#\#\#\#}P < 0.0001$) the anxiolytic effect of C2OHPDA (4 mg/kg, i.p.) and fluoxetine (Flx; 0.05 mg/kg; i.p.) (Figure 5b).

3.5.3 | Involvement of 5-HT_1 and 5-$HT_{2A/2C}$ system

Pizotifene did not reduce the anxiolytic effect of C2OHPDA (4 mg/kg, i.p.). However, pizotifene reduced ($^{\#\#\#\#}P < 0.0001$) the anxiolytic effect of fluoxetine (Flx; 0.05 mg/kg; i.p.) (Figure 5c).

3.6 | Molecular docking

All simulations performed with 5-HT_{2A} and 5-HT_{3A} receptors showed RMSD values lower than 2.0 Å and affinity energy lower than −6.0 kcal/mol (reference values). The best pose of the C2OHPDA-5HT_{2A}R, risperidone-5HT_{2A}R, C2OHPDA-5HT_{3A}, and granisetron-5HT_{3A}

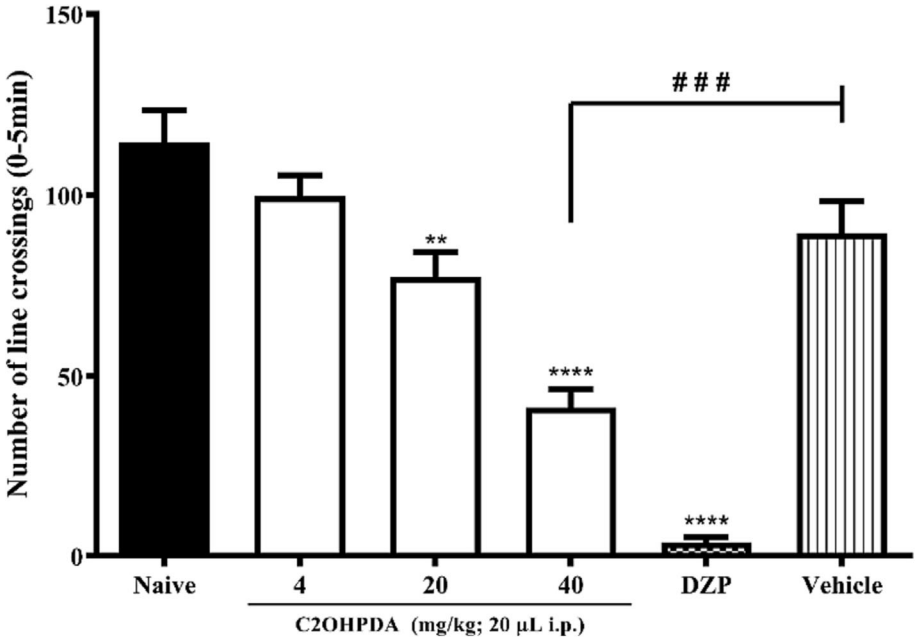

FIGURE 3 Effect of C2OHPDA chalcone under the locomotor behavior of zebrafish (*Danio rerio*) adult in the open-field test (0–5 min). Dzp—diazepam (4 mg/kg, 20 µL; i.p.); vehicle—(DMSO 3%; 20 µL; i.p.). Values represent the mean ± standard error of the mean for six animals/group; ANOVA followed by Tukey $^{****}P < 0.0001$, $^{**}P < 0.01$, $^{*}P < 0.05$ versus naive; $^{\#}P < 0.05$ versus vehicle.

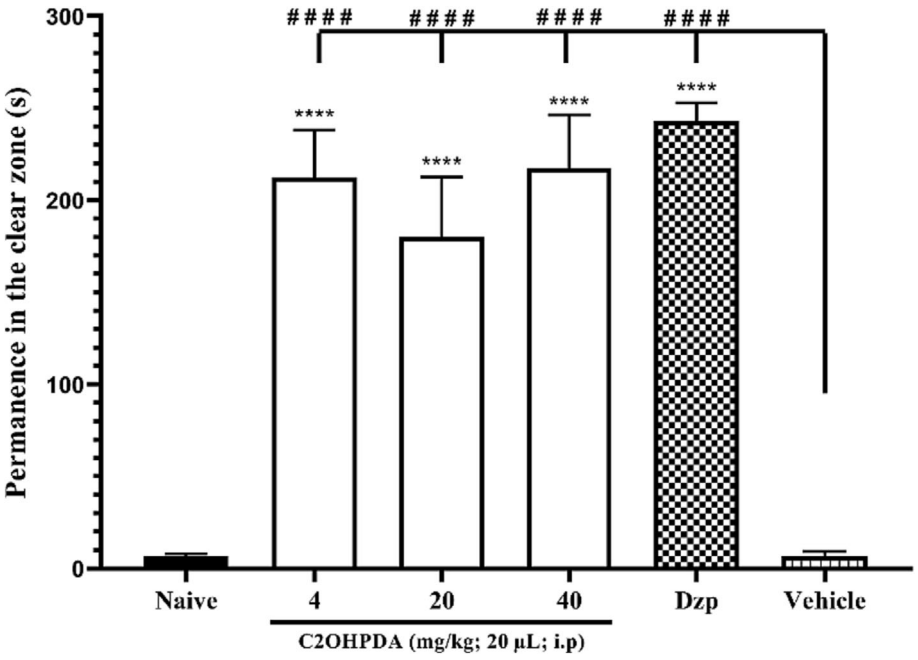

FIGURE 4 Effect of C2OHPDA chalcone on adult zebrafish in the Light & Dark Test (0–5 min). Dzp—diazepam (4 mg/kg, 20 µL; i.p.); vehicle—(DMSO 3%; 20 µL; i.p.). Values represent the mean ± standard error of the mean for six animals/group; ANOVA followed by Tukey $^{****}P < 0.0001$, $^{***}P < 0.001$ versus naive; $^{\#\#\#\#}P < 0.0001$; $^{\#\#\#}P < 0.001$ versus vehicle.

complexes showed RMSD in the order of 1907, 1628, 1733, and 1664 Å, respectively.

Analyzing the affinity energy, it was observed that the chalcone C2OHPDA presented against the 5-HT_{2A}R channel the value of −8.7 kcal/mol and against the 5-HT_{3A} channel the value of −9.1 kcal/mol, and the redocking simulations of the inhibitors co-crystallized risperidone (5-HT_{2A}R) and granisetron (5-HT_{3A}) showed affinity energy in the order of −11.1 kcal/mol and −10.9 kcal/mol respectively, thus validating the simulations performed.

Regarding interactions, it was possible to identify that the C2OHPDA-5HT_{2A}R complex is formed by five hydrophobic interactions involving the apolar side chain of residues Ile 163A (3.47 Å), Phe 243A (3.61 Å), Phe 332A (3.51 Å), Phe 339A (3.63 and 3.75 Å), two H-bonds, one *strong* with the uncharged polar side chain residue Thr 160A (2.78 Å), an average with the uncharged polar side chain residue Ser 159A (3.07 Å), in addition to of two p-Stacking interactions with the nonpolar side chain of aromatic residues Trp 336A (4.90 Å) and Phe 340A (4.89 Å) (Figure 6).

The C2OHPDA-5HT_{3A} complex is formed by five hydrophobic interactions, four with the nonpolar side chain of residues Ile 44E (3.88 Å), Trp 63E (3.68 Å), Phe 199A (3.94 Å), and Ile 201A (3.55 Å), one involving

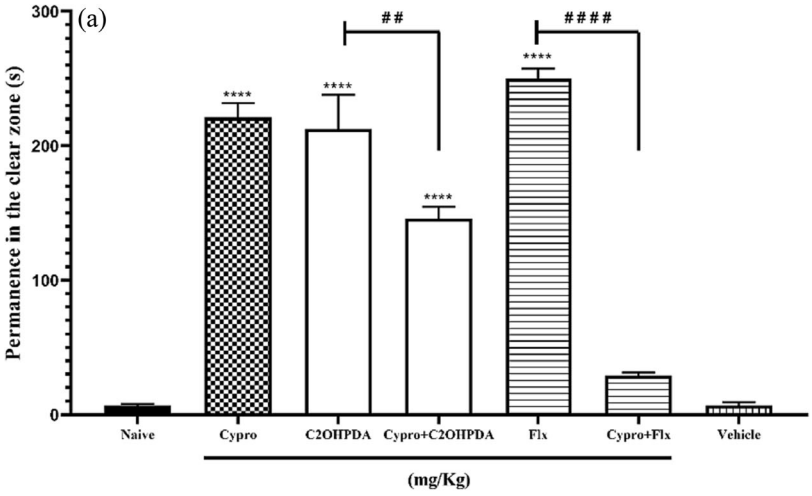

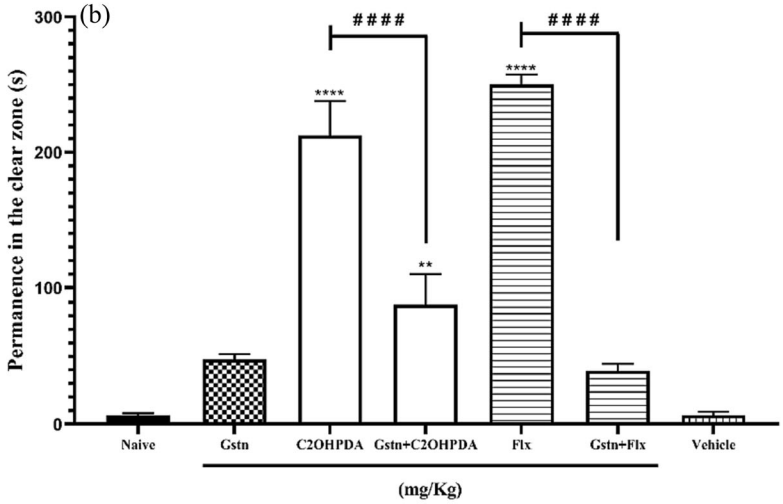

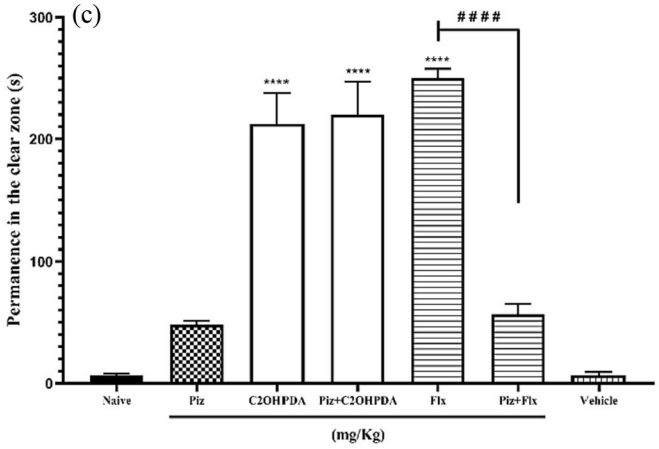

FIGURE 5 Treatment effect of cyproheptadine (a), granisetron (b), and pizotifene (c) under the anxiolytic effect of C2OHPDA chalcone in the Light & Dark Test. Cypro - cyproheptadine; GSTN—granisetron; PIZ—pizotifene; FLX—fluoxetine; vehicle—(DMSO 3%). Values represent the mean ± standard error of the mean for 6 animals/group; ANOVA followed by Tukey $^{****}P < 0.0001$ versus naive or vehicle; $^{\#\#\#\#}P < 0.0001$ versus C2OHPDA.

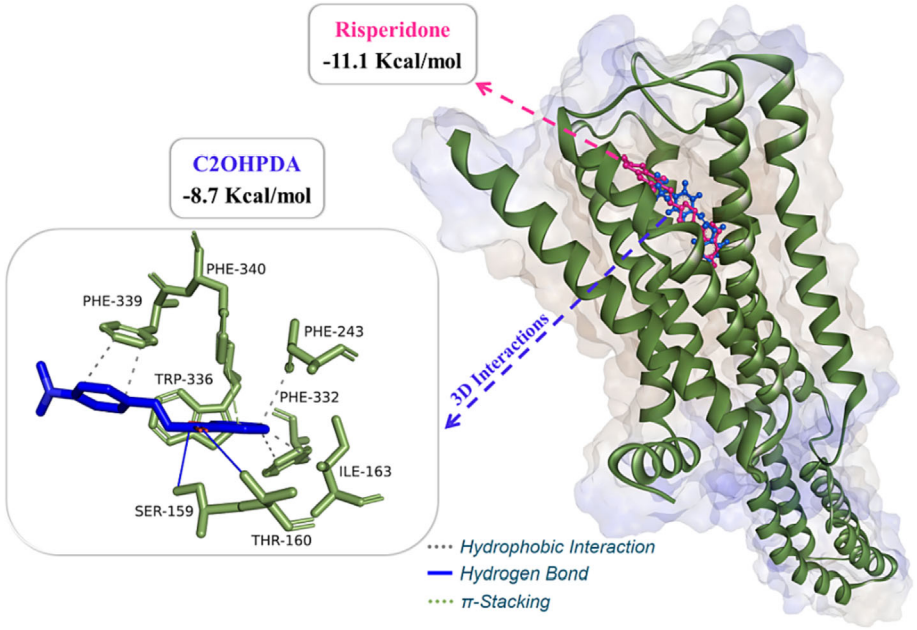

FIGURE 6 Interaction complex between the 5-HT_{2A}R receptor, the chalcone C2OHPDA and the co-crystallized inhibitor risperidone.

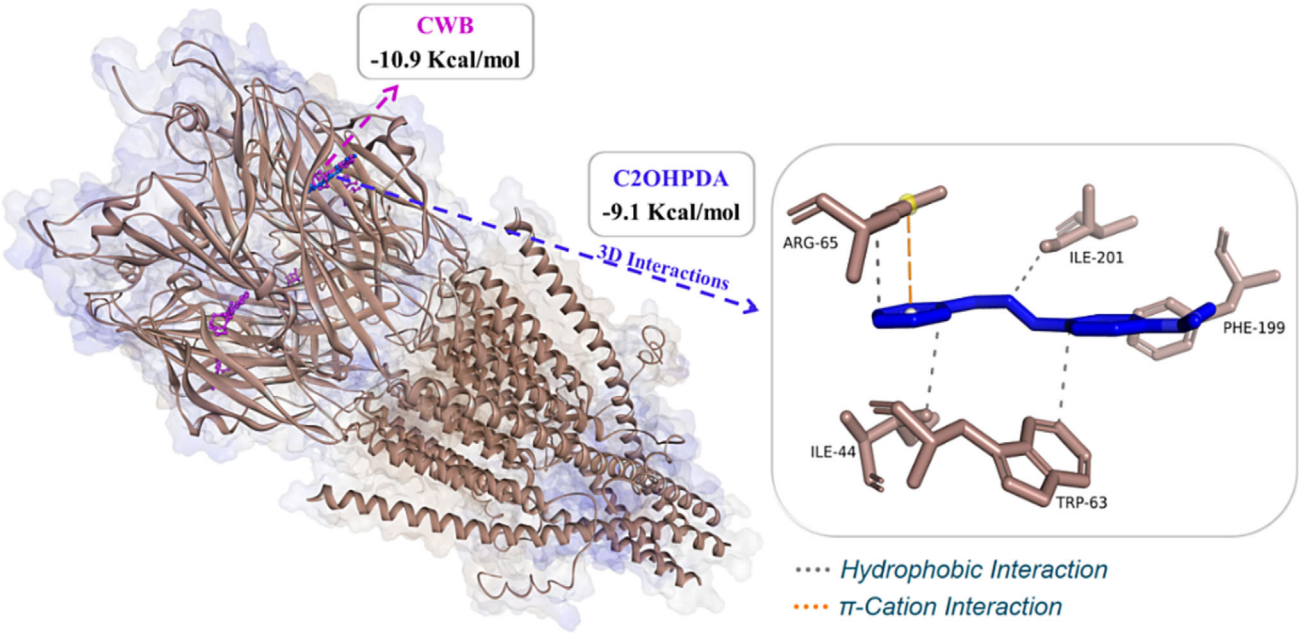

FIGURE 7 Complex of interaction between the 5-HT_{3A} receptor, the chalcone C2OHPDA and the co-crystallized inhibitor granisetron (CWB).

the basic side chain residue Arg 65E (3.59 Å) and a p-Cation-like interaction with the primary side chain residue Arg 65E (4.21 Å) (Figure 7).

3.7 | Physicochemical properties and drug-likeness assessment

The calculated physicochemical properties are listed in Table 2 and can be visually inspected on the bioavailability radar (Figure 8), which combines the criteria of Lipinski's "rule of five" (Pfizer) and Veber's rule (GSK). C2OHPDA has an optimized molecular size (MW = 267.33 g/mol) and a good lipid-soluble balance (logP = 4.34), according to Lipinski's rule, which allows a good passive diffusion in the cellular lipid bilayer, a value that corroborates with moderate solubility in an aqueous medium (logS = −3.35). It is interesting to note that the calculated polar surface area (TPSA) of 40.54 $Å^2$ is within the ideal spectrum predicted by

TABLE 2 Physicochemical properties and drug-likeness profile of the C2OHPDA.

Physicochemical property	Value	Source
Molecular weight	267.33 g/mol	ChemAxon
logP	4.34	ChemAxon
WlogP	3.25	Wildman and Crippen
HBA	2	ChemAxon
HBD	1	ChemAxon
Rotb	4	ChemAxon
TPSA	40.54 Å^2	ChemAxon
pKa (most acid)	7.20	ChemAxon
pKa (most basic)	4.73	ChemAxon
logD	3.93	ChemAxon
logS	−3.35	ChemAxon
Lipinski (Pfizer) rule	Yes; 0 violation	Lipinski
Veber (GSK) rule	Yes; 0 violation	Veber
CNS MPO (Pfizer) score	4.11	ChemAxon

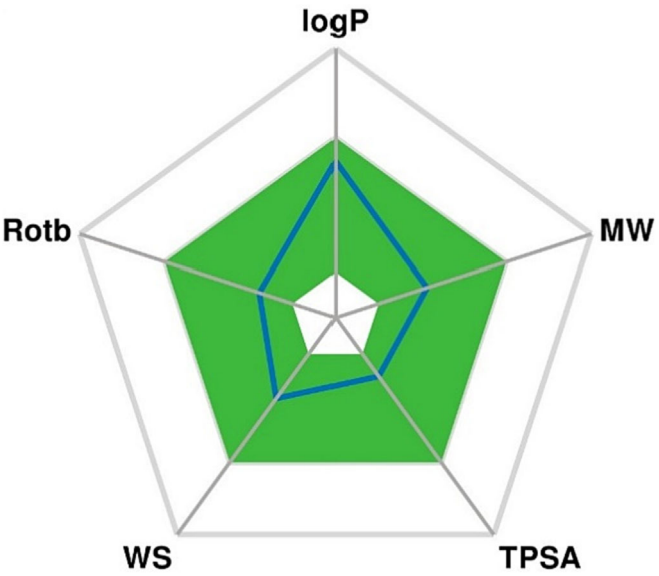

FIGURE 8 Lipinski and Veber rules bioavailability radar.

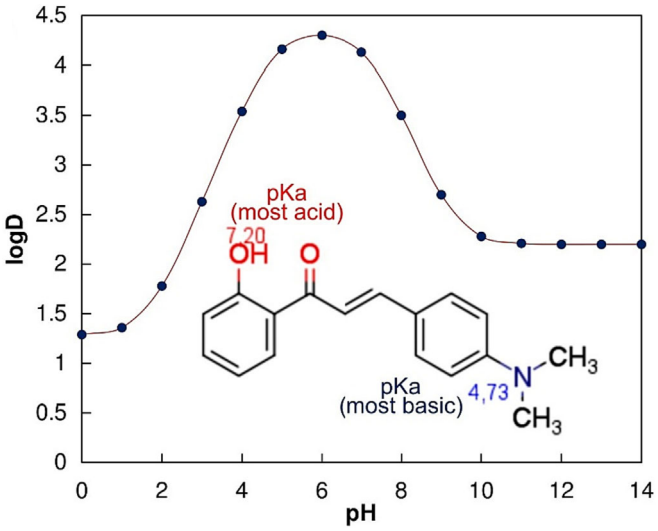

FIGURE 9 pH-dependent lipophilicity.

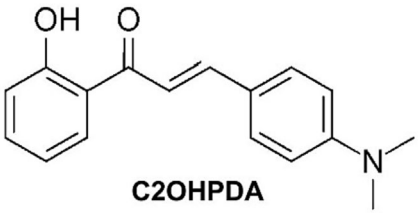

	Value	T0
logP score	4.34	0.33
logD score	3.93	0.03
MW score	267.33	1
TPSA score	40.54	1
HBD score	1	0.75
pKa score	4.73	1
CNS MPO score		4.11

FIGURE 10 Drug-likeness score by the CNS MPO algorithm (Pfizer).

Veber's rule for good cell permeability and is related to the number of H-bond receptors and donors from the rule of Lipinski (HBA ≤ 10 and HBD ≤ 5). At the same time, the four rotating bonds (Rotb) reflect its semiplanar structure, which allows a good balance of interactions with biological receptors.

When evaluating the pH-dependent properties, it is possible to observe that the C2OHPDA tends to a shifted equilibrium toward the increase of its lipophilicity due to the more basic center formed by its *para*-dimethylamino group at acid pH levels (pKa = 4.73) and tends to a more water-soluble microspecies with increasing pH, since logD at pH 7.4 in the order of 3.93 is associated with the presence of species with a negative charge in its *ortho*-hydroxy group (pKa = 7.20) (Figure 9).

The physicochemical properties were applied to the CNS MPO algorithm, from Pfizer, to promote the C2OHPDA to an optimized lead substance (lead likeness) as an active drug in the CNS. This model estimates the oral bioavailability (Figure 10), where the obtained score of 4.11 shows a good alignment of the physicochemical properties, presenting a good drug-likeness profile of this substance.

3.8 | ADME forecast assessment

The results of the consensus prediction of absorption, distribution, metabolism, and excretion (ADME) between the SwissADME and ADMETlab v2.0 platforms are listed in Table 2 and show a good alignment with the MPO. Furthermore, the CNS MPO score >4 demonstrates that the compound satisfies the pharmacokinetic attributes and follows the ADME prediction. Through the obtained results, it is possible to observe that the C2OHPDA has high passive permeability (Papp), where the predicted value of 1.5×10^{-5} cm/s for the in vitro model of Madin–Darby canine kidney cell line (MDCK) allows that the substance can penetrate the blood–brain barrier (BBB), especially intestinal epithelial cells, which guarantees high human intestinal absorption (HIA) and CNS activity, as well as showing the alignment between logP and TPSA of the Pfizer dataset (WlogP > 3.0 and TPSA ≤ 75 Å^2) (Figure 11) and the BOILED-Egg predictive model of the SwissADME platform (0.4 < WlogP ≤ 6.0 and TPSA ≤ 79 Å^2). In addition, the substance tested negative for P-glycoprotein substrate (P-gp), as a factor that justifies the optimal oral bioavailability (F) evaluated by the platforms, resulting in a volume of distribution (VD) that allows interaction and uniform distribution between blood plasma and different biological tissues (0.538 L/kg).

When the metabolism is evaluated through the enzymatic isoforms of cytochrome P450 (CYP450), it is possible to observe that the C2OHPDA is an inhibitor of the studied isoforms (1A2, 2C9, 2C19, 2D6, and 3A4), which changes the plasma concentration of co-administered and substrates of this species (Table 2). Furthermore, the site of metabolism prediction (SOMP) showed that the terminal carbons of the *para*-methylamino group are susceptible to N-dealkylation, forming an idiosyncratic secondary metabolite by metabolic activation. However, the lipophilic active principle of the substance guarantees a low metabolic clearance ($CL_{int,u}$ = 9744 mL/min/kg) and a longer half-life in the human body (Table 3).

3.9 | Quantum chemical calculations

The optimized structure of the title chalcone obtained at B3LYP/6-311++G(d,p) level of theory in the gas phase is shown in Figure 12. From this optimized structure, the molecular electrostatic potential was computed at the same computational level, and it is shown in Figure 13. The red-colored regions correspond to a negative charge distribution, the orange-to-yellow-colored regions to a partial negative charge distribution, the green-colored regions to a neutral charge distribution, the light blue colored-region to a partially favorable charge distribution, and the blue-colored areas to a positive charge distribution. According to Figure 13, the oxygen atoms of the hydroxyl groups have a red-colored charge distribution which agrees with the higher electronegativity of these atoms. The hydrogen atoms have a light, blue-colored charge distribution which means that these atoms have a partial positive charge. The hydrogen atoms bonded to the oxygen

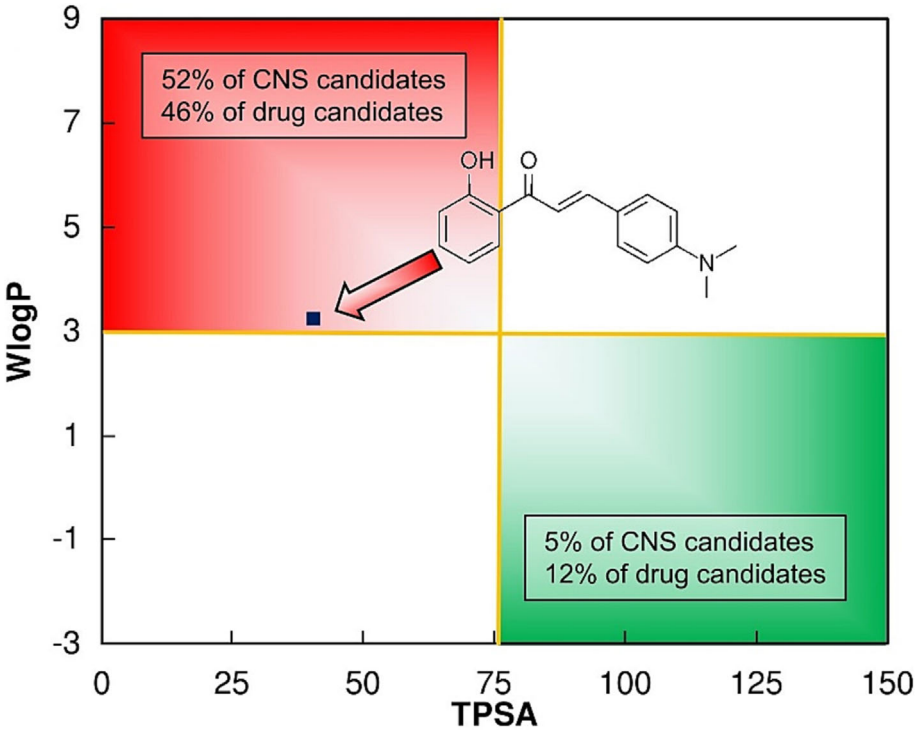

FIGURE 11 Graphic of the physical–chemical space of the C2OHPDA chalcone applied to the Pfizer dataset.

TABLE 3 ADME predicted properties by the in silico tools of the SwissADME server and in vitro similarity of the ADMETlab v2.0 server.

ADME property	SwissADME	ADMETlab v2.0[a]
Absorption		
Bioavailability (*F*)	0.55	−−−
P-gp substrate	No	−−−
HIA	High	−−−
Distribution		
VD	Not reported	0.538 L/kg
BBB permeation	Yes	1.5×10^{-5} cm/s (P_{app} MDCK)
Metabolism		
CYP1A2 inhibitor	Yes	+++
CYP2C9 inhibitor	Yes	++
CYP2C19 inhibitor	Yes	+++
CYP2D6 inhibitor	Yes	+
CYP3A4 inhibitor	Yes	++
Excretion		
$CL_{int,u}$	Not reported	9.744 mL/min/kg

[a]ADMETlab v2.0 predictive probability is converted to the symbols: "+++" or "++" as high probability of being toxic or defective, while "−−−" or "−−" represents low toxic risk or an appropriate result.

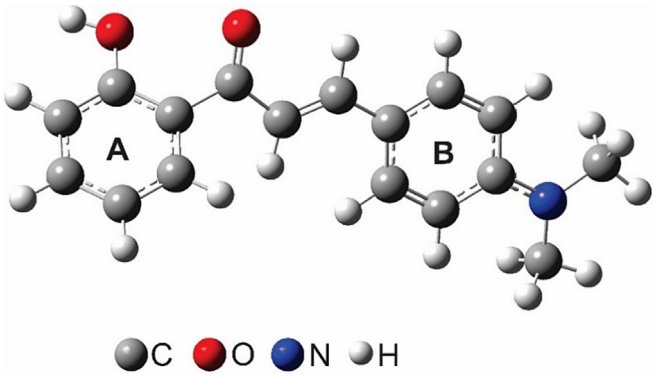

FIGURE 12 Optimized geometry obtained at B3LYP/6-311++G(d,p) level of theory in the gas phase.

and nitrogen atoms have a blue-colored charge distribution, showing that the partial positive charge is higher in these atoms. Finally, the molecular carbon skeleton has an orange-to-yellow colored charge distribution due to the π electronic density spread over the entire molecule. Hence, this chalcone can interact with other species using this electronic density as π-interactions.

Chalcones constitute the class of polyphenolic compounds, belonging to the family of flavonoids [49]. They have an α,β-unsaturated ketone system in their structure [50] with the presence of hydrogens that various functional groups can substitute, such as benzenes, halogens, aryls, hydroxyls and carboxylic [51], and the synthesis of new derivatives may occur, with several

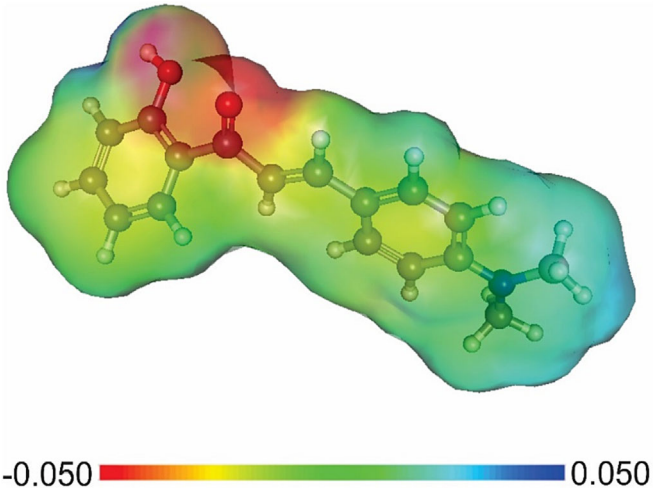

FIGURE 13 Molecular electrostatic potential obtained at B3LYP/6-311++G(d,p) level of theory in the gas phase.

associated pharmacological activities [52]. Anticonvulsant [53], antimicrobial, anticancer, and anxiolytic [54] effects have already been reported.

Zebrafish is very useful for testing the toxicity of a given drug, as it is cheaper, requires less time and requires a small amount of the substance in question, combining the scale and performance of in vitro tests with the physiological complexity of in vivo testing [55]. With the results obtained, it was observed that the C2OHPDA was not toxic to zebrafish within 96 h, making it possible to select safe doses.

This animal model presents morphological, genetic, and behavioral similarities with mammals. It is useful in studying neurological and psychiatric diseases, as it exhibits a complexity of behaviors in the social, learning, memory, defensiveness and anxiety spheres [16]. Through changes in the animal's locomotor activity, it is possible to study neuromuscular diseases and the effectiveness of drugs that can interfere with the animal's locomotion process [56], such as anxiolytic drugs, to which zebrafish is reasonably susceptible, suffering reduction in their swimming movements [57]. Thus, through the open-field test, it was possible to evaluate the locomotor system of the animal, resulting in significant impairment in its motor coordination when treated with C2OHPDA at doses of 20 ($P < 0.01$ vs. naive) and 40 mg/kg ($P < 0.0001$ vs. naive), indicating a sedative effect on the CNS, requiring the light/dark test to assess its anxiolytic activity.

The light/dark test is used by neuroscience to assess the animal's behavior in the face of fear and anxiety. It occurs through the administration of anxiolytic drugs, which directly influence the increase of the zebrafish's permanence time in the clear compartment of the aquarium. In contrast, anxiogenic drugs decrease this permanence time. This behavioral pattern is linked to a tendency of the animal to seek

protection, stay in the dark zone, or explore a new environment, going to the light zone. The intraperitoneal administration of C2OHPDA, at doses of 4, 20, and 40 mg/kg, increased ($P < 0.0001$ vs. vehicle) the time of permanence of the animal in the clear zone of the aquarium, like the positive control diazepam, suggesting an anxiolytic effect. In a study, chalcones with methoxy, methyl, halogen, nitro, and dimethylamine groups in their constitution generally show anxiolytic activity [58], with the latter substituent present in the chalcone in question.

The interaction between the C2OHPDA and the 5-HT receptors (5-HTRs) of the serotonergic system involved with anxiety was investigated. The neurotransmitter serotonin (5-hydroxytryptamine) is produced in neurons and is related to the processes of learning, aggression, affection, fear, and anxiety [59]. Its receptors are distributed throughout the central and peripheral nervous system, more precisely in the regions of the brain related to anxiety and depression [60]. The anxiolytic activity of chalcone C2OHPDA was evaluated after pretreatment with cyproheptadine (5-HTR_{2A} antagonist), pizotifen (5-HTR_1 and 5-$HTR_{2A/2C}$ antagonist), and granisetron (5-$HTR_{3A/3B}$ antagonist). Fluoxetine was used as a positive control. The results showed no reversal of the anxiolytic effect of chalcone C2OHPDA in the group treated with pizotifen (5-HTR_1 and 5-$HTR_{2A/2C}$), since the animals remained longer in the clear region of the aquarium. However, pretreatment with cyproheptadine and granisetron significantly ($^{\#\#}P < 0.01$; $^{\#\#\#\#}P < 0.0001$) inhibited the anxiolytic effect of C2OHPDA, suggesting that the mechanism of action involves 5-HTR_{2A} and 5-$HTR_{3A/3B}$ receptors, the effect observed on the latter being more significant. In addition, all antagonists used were able to reverse the effect of fluoxetine.

Serotonin 5-HT2A receptors are widely distributed in the CNS and abnormalities in their structure and function are associated with drug dependence, schizophrenia, depression and anxiety [61]. These receptors are classified as metabotropic, being G protein-coupled, and excitatory, as they are related to the G_q/G_{11} signal transduction pathway [59]. The 5-HT_{2A} receptor has several ligands that induce different responses, such as the psychoactive substances cyproheptadine and risperidone [62, 63]. The risperidone binding site on the 5-HT_{2A}R channel is formed by Ser 131A, Trp 151A, Asp 155A, Val 156A, Ser 159A, Thr 160A, Ile 163A, Leu 228A, Ser 242A, Phe 243A, Phe 332A, Trp 336A, Phe 339A, Phe 340A, Leu 362A, Asn 363A, Val 366A, and Tyr 370A residues. Some of these residues and their respective conformations are very important for receptor activation, namely Ile 163A, Phe 332A, and Trp 336A [38]. Chalcone C2OHPDA complexes in the same region as the binding site of risperidone, interacting with residues of Chain A, having in common interactions with residues Ser 159A, Thr 160A, Ile 163A, Phe 243A, Phe 332A, Phe 339A, Trp 336A, and Phe 340A, being indicative of similar activity (Figure 10). According to the molecular electrostatic potential in Figure 11, these interactions occur due to the π electronic density spread over the molecular structure and the negative charge distributed over the oxygen atoms. Blockade of the 5-HT_{2A} receptor has already been investigated in some preclinical research and the activity observed was also an anxiolytic effect [62].

Dysfunctions in 5-HT_3R receptors are related to several psychiatric conditions, such as bipolarity, depression, and anxiety [64, 65]. Granisetron is known to be a highly selective, potent antagonist and irreversible blocker of serotonin 5-HT_3 receptors, in which the depletion of this neurotransmitter is related to an anxiogenic-like behavior [66, 67]. This is the only one of the receptors of this family that is not coupled to the G protein, being a ligand-controlled pentamer ion channel, known as ionotropic, permeable to Na^+, Ca^{2+}, and K^+ ions [59]. Its binding site with the 5-HT_{3A} channel is formed by Asp 42E, Val 43E, Ile 44E, Trp 63E, Tyr 64E, Arg 65E, Asn 101A, Tyr 126E, Thr 154A, Ser 155A, Trp 156A, Arg 169E, Asp 177E, Phe 199A, Ile 201A, Tyr 207A, and Glu 209A residues [39]. Some of these residues are extremely important and must be conserved, such as Trp156, Phe199, Tyr207, Trp63, Arg65, and Tyr126, as possible changes directly impact their binding to serotonin [39]. It was noted that the C2OHPDA complexes in the same region of the granisetron binding site (CWB) co-crystallized between the A and E chains, having in common interactions with residues Ile 44E, Trp 63E, Arg 65E, Phe 199A, and Ile 201A, indicating a similar action (Figure 11), but with greater affinity for this receptor, confirming what was previously observed in the mechanism test involving zebrafish. According to studies in mice, the deletion of the gene responsible for the 5-HT_3 receptor makes them naturally anxiolytic [68, 69], reinforcing the importance of the interaction between antagonists and this receptor, for the treatment of anxiety.

Pharmacokinetics evaluates the concentrations of a drug and/or its metabolites in the body, after administration and over time [70]. There are four processes that directly interfere with the pharmacokinetics of drugs, absorption, distribution, metabolism, and excretion (ADMET) [20]. The study of these parameters becomes essential in the initial phase of new drug development, as it reduces pharmacokinetic failures during the application of clinical research [71].

C2OHPDA was tracked by Lipinski's "rule of five" and by Veber's rule, which allow predicting the oral bioavailability of the compound [72]. The first is based on four physicochemical parameters, namely, molecular weight (MW ≤ 500 g/mol), octanol/water partition coefficient (logP ≤ 5), hydrogen bond acceptors (HBA ≤ 10), and bond donors of hydrogen (HBD ≤ 5); the second

evaluates several rotating bonds (Rotb ≤ 10) and the polarity (TPSA ≤ 140 Å^2) [46, 72]. Through the results obtained, the chalcone in question did not show any violation of the parameters contained in the rules used, having a lipid-soluble balance and an easiness to passively diffuse the cellular lipid bilayer, being characteristics that allow the administration of the drug orally.

A major challenge for the pharmaceutical industry is the discovery and development of drugs with action on the CNS, with a very low success rate, ranging from 7% to 8% [73]. In a recent study, a new CNS drug optimization technique, CNS MPO, was created to improve drug planning with activity in this region. It has a score ranging from 0 to 6, which is generated from six fundamental physicochemical parameters, logP ≤ 3, logD ≤ 2, MW ≤ 360 g/mol, 40 < TPSA ≤ 90 Å^2, HBD < 1, and pKa ≤ 8. A CNS MPO score ≥4 indicates good pharmacokinetic alignment [74]. Thus, the chalcone C2OHPDA satisfied most of the drug-likeness criteria, showing a high passive permeability (P_{app}), a low risk of efflux by P-glycoprotein (P-gp) and a low clearance of the unbound molecular fraction in the system liver ($CL_{int,u}$). Through an alignment between logP and TPSA and the predictive model of BOILED-Egg, it was possible to observe that the substance can cross the blood–brain barrier (BBB) and intestinal epithelial cells (IAH), in addition to testing negative for the glycoprotein P, justifying its excellent oral bioavailability (F), an important parameter due to the preference of the oral route over the others, for presenting safety, economy, convenience, and comfort for the patient [75, 76]. Furthermore, the C2OHPDA belongs to the class of compounds with neutral charge at physiological pH (approximately pH 7.4) and nonviolating the criteria of Lipinski's rule, which reflects its bioavailability score (F) in the order of 0.55 [77].

The good pharmacokinetic performance of C2OHPDA can also be explained by the good alignment between its lipophilicity and polarity parameters, properties commonly used in the literature to mediate drug absorption and permeability [75, 78]. In the Pfizer dataset used to optimize the physical–chemical space of the CNS MPO algorithm, about 52% of CNS active drug candidates occupied the graph quadrant of logP > 3 and TPSA ≤ 75 Å^2, physical–chemical space occupied by the C2OHPDA, showing that the activity in the CNS is likely and feasible according to in vitro parameters.

The oxidative metabolism of drugs involves different isoforms of cytochrome P450 (CYP450), being responsible for more than 90% of the enzymatic reactions in the body. This process can be explained by the action of isoforms 1A2, 2C9, 2C19, 2D6, and 3A4, in which the largest fraction of P450 reactions is catalyzed by isoform 3A [79]. With the results obtained, it is possible to notice the influence of the evaluated CYP450 isoforms on the low clearance rate of C2OHPDA ($CL_{int,u}$ = 9744 mL/min/kg) and, consequently, on the high half-life. The prediction of sites of metabolism (SOMP) showed that the *para*-dimethylamino substituent is subject to N-dealkylation reactions by the five isoforms, constituting a product that can cause liver damage (DILI) at high doses administered [80].

4 | CONCLUSIONS

The results of the present study revealed that C2OHPDA is not toxic to adult zebrafish (*Danio rerio*). A reduction in the locomotor activity of the animal was evidenced, and later, its anxiolytic effect was confirmed, being mediated by the serotonergic system (5-HT), with promising action on 5-HT_{2A} and 5-$HT_{3A/3B}$ receptors. The interaction of chalcone with the 5-HTR receptor was confirmed by the molecular docking study, in which the interaction was verified in the two targets evaluated, 5-HT_{2A}R and 5-HT_{3A}, but showing a greater affinity for the latter channel (−9.1 kcal/mol). The chalcone evaluated satisfied the physicochemical characteristics necessary for drugs with action in the CNS, having good performance in the brain. Its pharmacokinetics was based on the optimal bioavailability by the oral route due to its parameters of high passive permeability and low risk of efflux by P-glycoprotein. Furthermore, the chalcone C2OHPDA inhibited all cytochrome P-450 isoforms analyzed, in addition to being susceptible to forming an idiosyncratic secondary metabolite, which in high concentrations can be hepatotoxic.

AUTHOR CONTRIBUTIONS

Larissa Santos Oliveira: Investigation; formal analysis; writing—original draft. **Hélcio Silva dos Santos**: Co-supervision; writing—review and editing. **Antonio Wlisses da Silva**: Project administration; conceptualization. **Jane Eire Silva Alencar de Menezes**: Funding; formal analysis; writing—review and editing. **Maria Kueirislene Amâncio Ferreira**: Methodology; formal analysis. **Emmanuel Silva Marinho**: Software; formal analysis; writing—review and editing. **Francisco Wagner de Queiroz Almeida-Neto**: Methodology; formal analysis. **José Ivo Lima Pinto Filho**: Methodology; formal analysis. **Márcia Machado Marinho**: Methodology; formal analysis. **Emanuelle Machado Marinho**: Software; visualization. **Matheus Nunes da Rocha**: Software; visualization. **Walber Henrique Ferreira Ribeiro**: Methodology; formal analysis. **Jane Eire Silva Alencar de Menezes**: Supervision; funding; formal analysis; writing—review and editing.

ACKNOWLEDGMENTS

The authors thank Northeastern Center for the Application and Use of Nuclear Magnetic Resonance (CENAUREMN). The authors also thank the Centro

Nacional de Processamento de Alto Desempenho (CENAPAD) of the Federal University of Ceará (UFC) for the use of the Gaussian09 software package.

CONFLICT OF INTEREST STATEMENT

All authors have no conflicts of interest to declare with respect to the research, authorship, and/or publication of this work.

ORCID

Márcia Machado Marinho https://orcid.org/0000-0002-7640-2220

Hélcio Silva dos Santos https://orcid.org/0000-0001-5527-164X

REFERENCES

1. Da Silva Lima DC, Do Vale CR, Veéras JH, Bernardes A, Peérez CN, Chen-Chen L. Absence of genotoxic effects of the chalcone (*E*)-1-(2-hydroxyphenyl)-3-(4-methylphenyl)-prop-2-en-1-one and its potential chemoprevention against DNA damage using in vitro and in vivo assays. *PLoS ONE*. 2017;12(2):1-15. doi:10.1371/journal.pone.0171224
2. Ferreira MKA, Fontenelle ROS, Magalhães FEA, Bandeira PN, De Menezes JSEA, Dos Santos HS. Chalcones pharmacological potential: A brief review. *Rev Virtual Quim*. 2018;10(5):1455-1473. doi:10.21577/1984-6835.20180099
3. Wang G, Liu W, Gong Z, Huang Y, Li Y, Peng Z. Design, synthesis, biological evaluation and molecular docking studies of new chalcone derivatives containing diaryl ether moiety as potential anticancer agents and tubulin polymerization inhibitors. *Bioorg Chem*. 2020;95:103565. doi:10.1016/j.bioorg.2019.103565
4. Li J, Li D, Xu Y, et al. Design, synthesis, biological evaluation, and molecular docking of chalcone derivatives as anti-inflammatory agents. *Bioorg Med Chem Lett*. 2017;27(3):602-606. doi:10.1016/j.bmcl.2016.12.008
5. Rocha JE, Freitas TS, Xavier JC, et al. ADMET study, spectroscopic characterization and effect of synthetic nitro chalcone in combination with norfloxacin, ciprofloxacin, and ethidium bromide against *Staphylococcus aureus* efflux pumps. *Fundam Clin Pharmacol*. 2022;37(1):163-173. doi:10.1111/fcp.12830
6. Vanangamudi G, Subramanian M, Thirunarayanan G. Synthesis, spectral linearity, antimicrobial, antioxidant and insect antifeedant activities of some 2,5-dimethyl-3-thienyl chalcones. *Arab J Chem*. 2017;10:S1254-S1266. doi:10.1016/j.arabjc.2013.03.006
7. Mohamad AS, Akhtar MN, Zakaria ZA, et al. Antinociceptive activity of a synthetic chalcone, flavokawin B on chemical and thermal models of nociception in mice. *Eur J Pharmacol*. 2010;647(1-3):103-109. doi:10.1016/j.ejphar.2010.08.030
8. Viana GSB, Bandeira MAM, Matos FJA. Analgesic and antiinflammatory effects of chalcones isolated from *Myracrodruon urundeuva* Allemão. *Phytomedicine*. 2003;10(2-3):189-195. doi:10.1078/094471103321659924
9. Beyhan N, Kocyigit-Kaymakcioglu B, Gümrü S, Aricioglu F. Synthesis and anticonvulsant activity of some 2-pyrazolines derived from chalcones. *Arab J Chem*. 2017;10:S2073-S2081. doi:10.1016/j.arabjc.2013.07.037
10. Borchhardt DM, Mascarello A, Chiaradia LD, et al. Biochemical evaluation of a series of synthetic chalcone and hydrazide derivatives as novel inhibitors of cruzain from trypanosoma cruzi. *J Braz Chem Soc*. 2010;21(1):142-150. doi:10.1590/S0103-50532010000100021
11. Jamal H, Ansari WH, Rizvi SJ. Evaluation of chalcones—a flavonoid subclass, for, their anxiolytic effects in rats using elevated plus maze and open field behaviour tests. *Fundam Clin Pharmacol*. 2008;22(6):673-681. doi:10.1111/j.1472-8206.2008.00639.x
12. Dourado DM, Rolim JA, Dourado D. Ansiedade e depressão em cuidador familiar de pessoa com transtorno mental. *ECOS-Estudos Contemporâneos da Subjetividade*. 2018;8(1):153-167.
13. World Health Organization. *Depression and Other Common Mental Disorders: Global Health Estimates*. World Health Organization; 2017:1-24. CC BY-NC-SA 3.0 IGO.
14. Goularte JF, Serafim SD, Colombo R, Hogg B, Caldieraro MA, Rosa AR. COVID-19 and mental health in Brazil: psychiatric symptoms in the general population. *J Psychiatr Res*. 2021;132:32-37. doi:10.1016/j.jpsychires.2020.09.021
15. Griffin CE, Kaye AM, Rivera Bueno F, Kaye AD. Benzodiazepine pharmacology and central nervous system-mediated effects. *Ochsner J*. 2013;13(2):214-223.
16. Basnet RM, Zizioli D, Taweedet S, Finazzi D, Memo M. Zebrafish larvae as a behavioral model in neuropharmacology. *Biomedicine*. 2019;7(1):23. doi:10.3390/BIOMEDICINES7010023
17. Cassar S, Adatto I, Freeman JL, et al. Use of zebrafish in drug discovery toxicology. *Chem Res Toxicol*. 2020;33(1):95-118. doi:10.1021/acs.chemrestox.9b00335
18. Sieber S, Grossen P, Bussmann J, et al. Zebrafish as a preclinical in vivo screening model for nanomedicines. *Adv Drug Deliv Rev*. 2019;151–152:152-168. doi:10.1016/j.addr.2019.01.001
19. Khanna I. Drug discovery in pharmaceutical industry: productivity challenges and trends. *Drug Discov Today*. 2012;17(19-20):1088-1102. doi:10.1016/j.drudis.2012.05.007
20. Fan J, De Lannoy IAM. Pharmacokinetics. *Biochem Pharmacol*. 2014;87(1):93-120. doi:10.1016/j.bcp.2013.09.007
21. Pinzi L, Rastelli G. Molecular docking: shifting paradigms in drug discovery. *Int J Mol Sci*. 2019;20(18):4331. doi:10.3390/ijms20184331
22. Wan H. What ADME tests should be conducted for preclinical studies? *ADMET DMPK*. 2013;1(3):19-28. doi:10.5599/admet.1.3.9
23. Magalhães FEA, De Sousa CÁPB, Santos SAAR, et al. Adult zebrafish (*Danio rerio*): an alternative behavioral model of formalin-induced nociception. *Zebrafish*. 2017;14(5):422-429. doi:10.1089/zeb.2017.1436
24. Ekambaram SP, Perumal SS, Pavadai S. Anti-inflammatory effect of *Naravelia zeylanica* DC via suppression of inflammatory mediators in carrageenan-induced abdominal oedema in zebrafish model. *Inflammopharmacology*. 2017;25(1):147-158. doi:10.1007/s10787-016-0303-2
25. Amali MO, Atunwa SA, Aiyelero OM, Omotesho QA. Assessment of anxiolytic potential and acute toxicity study of *Combretum micranthum* G. Don. leaves (Combretaceae). *IBRO Rep*. 2019;7:42. doi:10.1016/j.ibror.2019.09.085
26. Arellano-Aguilar O, Solis-Angeles S, Serrano-García L, Morales-Sierra, E. Mendez-Serrano, A. Montero-Montoya R. Use of the zebrafish embryo toxicity test for risk assessment purpose: case study. vol. 9. 2015.
27. Gebauer DL, Pagnussat N, Piato ÂL, Schaefer IC, Bonan CD, Lara DR. Effects of anxiolytics in zebrafish: similarities and differences between benzodiazepines, buspirone and ethanol. *Pharmacol Biochem Behav*. 2011;99(3):480-486. doi:10.1016/j.pbb.2011.04.021
28. Lima JD, Ferreira MK, Sales KV, et al. Diterpene Sonderianin isolated from *Croton blanchetianus* exhibits acetylcholinesterase inhibitory action and anxiolytic effect in adult zebrafish (*Danio rerio*) by 5-HT system. *J Biomol Struct Dyn*. 2022;40(24):13625-13640. doi:10.1080/07391102.2021.1991477
29. Huey R, Morris GM, Forli S. Using AutoDock 4 and AutoDock vina with AutoDockTools: a tutorial. 2012.
30. Trott O, Olson AJ. AutoDock Vina: improving the speed and accuracy of docking with a new scoring function, efficient optimization, and multithreading. *J Comput Chem*. 2010;31(2):455-461. doi:10.1002/jcc.21334

31. Biovia DS. Discovery Studio Modeling Environment, Release 2017, San Diego. Dassault Systèmes 2016. 2016.
32. Allouche A. Software news and updates Gabedit—a graphical user interface for computational chemistry softwares. *J Comput Chem*. 2012;32:174-182. doi:10.1002/jcc
33. Frisch, M.J.; Trucks, G.W.; Schlegel HB. S, G.E.; Robb, M.A.; Cheeseman, J.R.; Scalmani, G.; Barone, V.; Mennucci B., Petersson, G.A.; Nakatsuji, H.; Caricato, M.; Li, X.; Hratchian, H.P.; Izmaylov AF., Bloino, J.; Zheng, G.; Sonnenberg, J.L.; Hada, M.; Ehara, M.; Toyota, K.; Fukuda R., Hasegawa, J.; Ishida, M.; Nakajima, T.; Honda, Y.; Kitao, O.; Nakai, H.; Vreven T., Montgomery, J.A., Jr.; Peralta, J.E.; Ogliaro, F.; Bearpark, M.; Heyd JJ. B, et al. Gaussian 09, Revision A.02 2009.
34. Csizmadia P. MarvinSketch and MarvinView: molecule applets for the World Wide Web, 2019. 10.3390/ecsoc-3-01775.
35. DeLano WL. *The PyMOL Molecular Graphics System, Version 2.3*. Schrödinger LLC; 2020.
36. Pettersen EF, Goddard TD, Huang CC, et al. UCSF Chimera—a visualization system for exploratory research and analysis. *J Comput Chem*. 2004;25(13):1605-1612. doi:10.1002/jcc.20084
37. Becke AD. Density-functional thermochemistry. I. The effect of the exchange-only gradient correction. *J Chem Phys*. 1992;96(3):2155-2160. doi:10.1063/1.462066
38. Kimura KT, Asada H, Inoue A, et al. Structures of the 5-HT 2A receptor in complex with the antipsychotics risperidone and zotepine. *Nat Struct Mol Biol*. 2019;26(2):121-128. doi:10.1038/s41594-018-0180-z
39. Basak S, Gicheru Y, Kapoor A, Mayer ML, Filizola M, Chakrapani S. Molecular mechanism of setron-mediated inhibition of full-length 5-HT3A receptor. *Nat Commun*. 2019;10(1):3225. doi:10.1038/s41467-019-11142-8
40. Morris GM, Huey R, Lindstrom W, et al. AutoDock4 and AutoDockTools4: automated docking with selective receptor flexibility. *J Comput Chem*. 2009;30(16):2785-2791.
41. Yan J, Zhang G, Pan J, Wang Y. α-Glucosidase inhibition by luteolin: kinetics, interaction and molecular docking. *Int J Biol Macromol*. 2014;64:213-223. doi:10.1016/j.ijbiomac.2013.12.007
42. Marinho EM, Batista de Andrade Neto J, Silva J, et al. Virtual screening based on molecular docking of possible inhibitors of Covid-19 main protease. *Microb Pathog*. 2020;148:104365. doi:10.1016/j.micpath.2020.104365
43. Yusuf D, Davis AM, Kleywegt GJ, Schmitt S. An alternative method for the evaluation of docking performance: RSR vs RMSD. *J Chem Inf Model*. 2008;48(7):1411-1422. doi:10.1021/ci800084x
44. Shityakov S, Förster C. In silico predictive model to determine vector-mediated transport properties for the blood–brain barrier choline transporter. *Adv Appl Bioinforma Chem AABC*. 2014;7:23-36. doi:10.2147/AABC.S63749
45. Imberty A, Hardman KD, Carver JP, Perez S. Molecular modelling of protein-carbohydrate interactions. Docking of monosaccharides in the binding site of concanavalin A. *Glycobiology*. 1991;1(6):631-642. doi:10.1093/glycob/1.6.631
46. Da Rocha MN, Marinho ES, Marinho MM, Dos Santos HS. Virtual screening in pharmacokinetics, bioactivity, and toxicity of the amburana cearensis secondary metabolites. *Biointerface Res Appl Chem*. 2022;12(6):8471-8491. doi:10.33263/BRIAC126.84718491
47. Veber DF, Johnson SR, Cheng H, Smith BR, Ward KW, Kopple KD. Molecular properties that influence the oral bioavailability of drug candidates. *J Med Chem*. 2002;45(12):2615-2623. doi:10.1021/jm020017n
48. Ritchie TJ, Ertl P, Lewis R. The graphical representation of ADME-related molecule properties for medicinal chemists. *Drug Discov Today*. 2011;16(1-2):65-72. doi:10.1016/j.drudis.2010.11.002
49. Sukumaran SD, Chee CF, Viswanathan G, et al. Synthesis, biological evaluation and molecular modelling of 2′-hydroxychalcones as acetylcholinesterase inhibitors. *Molecules*. 2016;21(7):1-10. doi:10.3390/molecules21070955
50. Zhuang C, Zhang W, Sheng C, Zhang W, Xing C, Miao Z. Chalcone: a privileged structure in medicinal chemistry. *Chem Rev*. 2017;117(12):7762-7810. doi:10.1021/acs.chemrev.7b00020
51. Jandial D, Blair C, Zhang S, Krill L, Zhang Y-B, Zi X. Molecular targeted approaches to cancer therapy and prevention using chalcones. *Curr Cancer Drug Targets*. 2014;14(2):181-200. doi:10.2174/1568009614666140122160515
52. Gomes MN, Muratov EN, Pereira M, et al. Chalcone derivatives: promising starting points for drug design. *Molecules*. 2017;22(8):1210. doi:10.3390/molecules22081210
53. Ferreira MKA, Da Silva AW, dos Santos Moura AL, et al. Chalcones reverse the anxiety and convulsive behavior of adult zebrafish. *Epilepsy Behav*. 2021;117:107881. doi:10.1016/j.yebeh.2021.107881
54. da Cunha Xavier J, Almeida-Neto FW, da Silva PT, et al. Structural characterization, electronic properties, and anxiolytic-like effect in adult zebrafish (*Danio rerio*) of cinnamaldehyde chalcone. *J Mol Struct*. 2020;1222:128954. doi:10.1016/j.molstruc.2020.128954
55. Garcia GR, Noyes PD, Tanguay RL. Advancements in zebrafish applications for 21st century toxicology. *Pharmacol Ther*. 2016;161:11-21. doi:10.1016/j.pharmthera.2016.03.009
56. Tatem KS, Quinn JL, Phadke A, Yu Q, Gordish-Dressman H, Nagaraju K. Behavioral and locomotor measurements using an open field activity monitoring system for skeletal muscle diseases. *J vis Exp*. 2014;(91):51785. doi:10.3791/51785
57. Khan KM, Collier AD, Meshalkina DA, et al. Zebrafish models in neuropsychopharmacology and CNS drug discovery. *Br J Pharmacol*. 2017;174(13):1925-1944. doi:10.1111/bph.13754
58. Higgs J, Wasowski C, Marcos A, et al. Chalcone derivatives: synthesis, in vitro and in vivo evaluation of their anti-anxiety, anti-depression and analgesic effects. *Heliyon*. 2019;5(3):e01376. doi:10.1016/j.heliyon.2019.e01376
59. Nowicki M, Tran S, Muraleetharan A, Markovic S, Gerlai R. Serotonin antagonists induce anxiolytic and anxiogenic-like behavior in zebrafish in a receptor-subtype dependent manner. *Pharmacol Biochem Behav*. 2014;126:170-180. doi:10.1016/j.pbb.2014.09.022
60. Villas-Boas GR, Lavorato SN, Paes MM, et al. Modulation of the serotonergic receptosome in the treatment of anxiety and depression: a narrative review of the experimental evidence. *Pharmaceuticals*. 2021;14(2):1-46. doi:10.3390/ph14020148
61. Zhang G, Stackman RW. The role of serotonin 5-HT2A receptors in memory and cognition. *Front Pharmacol*. 2015;6:225. doi:10.3389/fphar.2015.00225
62. Cohen H. Anxiolytic effect and memory improvement in rats by antisense oligodeoxynucleotide to 5-hydroxytryptamine-2A precursor protein. *Depress Anxiety*. 2005;22(2):84-93. doi:10.1002/da.20087
63. Amodeo DA, Jones JH, Sweeney JA, Ragozzino ME. Risperidone and the 5-HT_{2A} receptor antagonist M100907 improve probabilistic reversal learning in BTBR T + tf/J mice. *Autism Res*. 2014;7(5):555-567. doi:10.1002/aur.1395
64. Bétry C, Etiévant A, Oosterhof C, Ebert B, Sanchez C, Haddjeri N. Role of 5-HT3 receptors in the antidepressant response. *Pharmaceuticals*. 2011;4(4):603-629. doi:10.3390/ph4040603
65. Thompson AJ, Lummis SCR. The 5-HT3 receptor as a therapeutic target. *Expert Opin Ther Targets*. 2007;11(4):527-540. doi:10.1517/14728222.11.4.527
66. Gupta P, Khobragade S, Rajaram S, Shingatgeri V. Assessment of locomotion behavior in adult zebrafish after acute exposure to different pharmacological reference compounds. *Drug Dev Ther*. 2014;5(2):127. doi:10.4103/2394-2002.139626

67. Maximino C, da Silva AWB, Gouveia A, Herculano AM. Pharmacological analysis of zebrafish (*Danio rerio*) scototaxis. *Prog Neuro-Psychopharmacol Biol Psychiatry*. 2011;35(2):624-631. doi:10.1016/j.pnpbp.2011.01.006
68. Kelley SP, Bratt AM, Hodge CW. Targeted gene deletion of the 5-HT3A receptor subunit produces an anxiolytic phenotype in mice. *Eur J Pharmacol*. 2003;461(1):19-25. doi:10.1016/S0014-2999(02)02960-6
69. Bhatnagar S, Nowak N, Babich L, Bok L. Deletion of the 5-HT3 receptor differentially affects behavior of males and females in the Porsolt forced swim and defensive withdrawal tests. *Behav Brain Res*. 2004;153(2):527-535. doi:10.1016/j.bbr.2004.01.018
70. Leslie Escobar QF. Therapeutic drug monitoring and practical aspects of pharmacokinetics. *Rev Medica Clin Las Condes*. 2016;27(5):605-614. doi:10.1016/j.rmclc.2016.09.006
71. Daina A, Michielin O, Zoete V. SwissADME: a free web tool to evaluate pharmacokinetics, drug-likeness and medicinal chemistry friendliness of small molecules. *Sci Rep*. 2017;7:42717. doi:10.1038/srep42717
72. Asokkumar K, Prathyusha LT, Umamaheshwari M, et al. Design, ADMET and docking studies on some novel chalcone derivatives as soluble epoxide hydrolase enzyme inhibitors. *J Chil Chem Soc*. 2012;57(4):1442-1446. doi:10.4067/S0717-97072012000400022
73. Geerts H, Wikswo J, van der Graaf PH, et al. Quantitative systems pharmacology for neuroscience drug discovery and development: current status, opportunities, and challenges. *CPT Pharmacometrics Syst Pharmacol*. 2020;9(1):5-20. doi:10.1002/psp4.12478
74. Wager TT, Hou X, Verhoest PR, Villalobos A. Central nervous system multiparameter optimization desirability: application in drug discovery. *ACS Chem Nerosci*. 2016;7(6):767-775. doi:10.1021/acschemneuro.6b00029
75. Daina A, Zoete V. A BOILED-egg to predict gastrointestinal absorption and brain penetration of small molecules. *ChemMedChem*. 2016;11(11):1117-1121. doi:10.1002/cmdc.201600182
76. Alves LS, Da Silva PLN, Fonseca JR, Vaz MDT, Santo LRE. Análise de interação medicamentosa de prescrições médicas contendo antimicrobianos de uma drogaria privada de Minas Gerais. *JMPHC J Manag Prim Heal Care*. 2019;10:1-23. doi:10.14295/jmphc.v10i0.481
77. Martin YC. A bioavailability score. *J Med Chem*. 2005;48(9):3164-3170. doi:10.1021/jm0492002
78. Ghose AK, Herbertz T, Hudkins RL, Dorsey BD, Mallamo JP. Knowledge-based, central nervous system (CNS) lead selection and lead optimization for CNS drug discovery. *ACS Chem Nerosci*. 2012;3(1):50-68. doi:10.1021/cn200100h
79. Rendic S, Guengerich FP. Survey of human oxidoreductases and cytochrome P450 enzymes involved in the metabolism of xenobiotic and natural chemicals. *Chem Res Toxicol*. 2015;28(1):38-42. doi:10.1021/tx500444e
80. Yu K, Geng X, Chen M, et al. High daily dose and being a substrate of cytochrome P450 enzymes are two important predictors of drug-induced liver injury. *Drug Metab Dispos*. 2014;42(4):744-750. doi:10.1124/dmd.113.056267

How to cite this article: Santos Oliveira L, Kueirislene Amâncio Ferreira M, Wagner de Queiroz Almeida-Neto F, et al. Synthesis, molecular docking, ADMET, and evaluation of the anxiolytic effect in adult zebrafish of synthetic chalcone (*E*)-3-(4-(dimethylamino) phenyl)-1-(2-hydroxyphenyl)prop-2-en-1-one: An in vivo and in silico approach. *Fundam Clin Pharmacol*. 2023;1-17. doi:10.1111/fcp.12960